Chemical Science

ROYAL SOCIETY OF CHEMISTRY

EDGE ARTICLE

View Article Online
View Journal | View Issue

Cite this: *Chem. Sci.*, 2021, **12**, 1458

All publication charges for this article have been paid for by the Royal Society of Chemistry

Investigation on the reactivity of nucleophilic radiohalogens with arylboronic acids in water: access to an efficient single-step method for the radioiodination and astatination of antibodies†

Marion Berdal, [a] Sébastien Gouard, [a] Romain Eychenne, [ab] Séverine Marionneau-Lambot, [ae] Mikaël Croyal, [cd] Alain Faivre-Chauvet, [ae] Michel Chérel, [af] Joëlle Gaschet, [a] Jean-François Gestin *[a] and François Guérard *[a]

Easy access to radioiodinated and ^{211}At-labelled bio(macro)molecules is essential to develop new strategies in nuclear imaging and targeted radionuclide therapy of cancers. Yet, the labelling of complex molecules with heavy radiohalogens is often poorly effective due to the multiple steps and intermediate purifications needed. Herein, we investigate the potential of arylboron chemistry as an alternative approach for the late stage labelling of antibodies. The reactivity of a model precursor, 4-chlorobenzeneboronic acid (**1**) with nucleophilic iodine-125 and astatine-211 was at first investigated in aqueous conditions. In the presence of a copper(II) catalyst and 1,10-phenanthroline, quantitative radiochemical yields (RCYs) were achieved within 30 minutes at room temperature. The optimum conditions were then applied to a CD138 targeting monoclonal antibody (mAb) that has previously been validated for imaging and therapy in a preclinical model of multiple myeloma. RCYs remained high (>80% for ^{125}I-labelling and >95% for ^{211}At-labelling), and the whole procedure led to increased specific activities within less time in comparison with previously reported methods. Biodistribution study in mice indicated that targeting properties of the radiolabelled mAb were well preserved, leading to a high tumour uptake in a CD138 expressing tumour model. The possibility of divergent synthesis from a common modified carrier protein demonstrated herein opens facilitated perspectives in radiotheranostic applications with the radioiodine/^{211}At pairs. Overall, the possibility to develop radiolabelling kits offered by this procedure should facilitate its translation to clinical applications.

Received 18th September 2020
Accepted 23rd November 2020

DOI: 10.1039/d0sc05191h

rsc.li/chemical-science

1. Introduction

Astatine-211 is a radionuclide of high interest in nuclear medicine for targeted α-therapy, a promising modality for the treatment of disseminated cancers.[1,2] ^{211}At emits one high energy α particle (5.7 or 7.4 MeV) per decay, with an intermediate half-life of 7.21 h making it compatible with a broad spectrum of carrier compounds pharmacokinetics, from small organic molecules to heavy intact antibodies. Reports over the past two decades have shown its promising efficacy on the eradication of isolated cancer cells or small cell clusters with limited toxicity at preclinical and clinical stages.[3–6] On the other hand, several radioisotopes of iodine have long been considered of interest for therapeutic and imaging applications, the most representative being iodine-131 (β^- and γ emitter, $t_{1/2} = 8$ days), iodine-123 (γ emitter, $t_{1/2} = 13.2$ h), iodine-124 (β^+ emitter, $t_{1/2} = 4.18$ days) and iodine-125 (γ and Auger electrons, $t_{1/2} = 59.5$ days).[7]

Astatine and iodine are both halogens and neighbours in the periodic table and, therefore, they exhibit a number of similar properties. Consequently, most reactions known for radioiodine are applicable similarly with astatine. Radiolabelling approaches have long been limited to nucleophilic halogen (or isotope) exchange, and to the highly popular electrophilic halodestannylation.[8,9] These reactions are mainly used in order to form halo(hetero)aryl compounds, sp^2 carbon–halogen bonds being preferred for stability reasons over sp^3 carbon. Alternatively, promising nucleophilic strategies using the radiohalogen as a nucleophilic species (X^-) were recently reported, based on

[a]Université de Nantes, CNRS, Inserm, CRCINA, F-44000 Nantes, France. E-mail: francois.guerard@univ-nantes.fr
[b]Arronax GIP, Saint-Herblain, France
[c]CRNH-O, Mass Spectrometry Core Facility, F-44000 Nantes, France
[d]NUN, INRA, CHU Nantes, UMR 1280, PhAN, IMAD, CRNH-O, F-44000 Nantes, France
[e]Department of Nuclear Medicine, CHU Nantes, Nantes, France
[f]ICO-René Gauducheau, Saint-Herblain, France

† Electronic supplementary information (ESI) available. See DOI: 10.1039/d0sc05191h

aryliodonium salts or arylboronic acids/esters precursors that provided high radiochemical yields (RCYs) on a broad scope of substrates.[10–12]

The availability of efficient nucleophilic radiolabelling approaches are in several aspects desirable. First of all, they avoid the use of electrophilic species and oxidizing conditions required for their formation that may alter the substrate or lead to side reactions. Additionally, these approaches exhibit advantages in the practical point of view: on the one hand, iodine radioisotopes are available commercially as sodium iodide solutions, ready to be used in nucleophilic reactions without a reduction step. On the other hand, the nucleophilic At^- species is much easier to produce since it is stable in reducing media over a broad pH range, whereas the electrophilic At^+ species exists only in a small pH and redox potential domain.[13] Better procedure robustness using nucleophilic astatine is thus expected in comparison with electrophilic approaches in which overoxidized non-reactive At species may negatively impact RCYs.

The first efficient approach for radiolabelling proteins with ^{211}At, which remains also the most widely used so far, is a two-step procedure based on the radiosynthesis of an intermediate prosthetic group, *N*-[^{211}At]succinimidylastatobenzoate ([^{211}At]SAB), *via* electrophilic astatodestannylation of the corresponding aryltrialkylstannane precursor (Scheme 1a),[14] similarly to the analogous procedure that had previously been developed for radioiodination.[15] To overcome issues with the use of electrophilic astatine and to eliminate the need of toxic organotin agents, we recently revisited this approach using nucleophilic astatine or iodine and an aryliodonium salt precursor (Scheme 1b).[16] On the other hand, a single-step strategy was developed by Lindegren *et al.*, for which the precursor is grafted to the antibody prior to the radiolabelling, saving time and increasing RCYs compared to two-step strategies (scheme 1c).[17,18] It is however still based on the previous electrophilic destannylation reaction and, although efficient for astatination, it cannot be applied for radioiodination since electrophilic radioiodine would react competitively with tyrosine and histidine residues, leading to suboptimal *in vivo* stability.[19] This issue does not exists in the case of astatine since electrophilic astatine cannot react with tyrosines or histidines unless very drastic conditions are applied.[20–22] Similarly, the one-step approach based on boron clusters which provides improved *in vivo* stability of radiolabelling, but can dramatically alter antibody biodistribution (Scheme 1d),[23,24] is also not applicable to radioiodination since it requires the electrophilic halogen species that may, again, react with tyrosines and histidine residues.

This incompatibility of use with radioiodine is a hurdle to the development of radiotheranostic antibodies based on the ^{211}At/^{123,124}I pairs. The concept of radiotheranostic pharmaceuticals is based on the use of a unique compound to perform both imaging and therapy,[25,26] and is considered as a promising approach in personalized therapy.

In this context, it appears essential to develop late stage radiohalogenation approaches applicable to proteins with both iodine and astatine radioisotopes. This implies the use of nucleophilic halogens in order to avoid issues inherent to electrophilic approaches discussed above. Previously reported nucleophilic astatination reactions require elevated temperatures, which is not compatible with proteins.[10,27,28]

Interestingly, boron reagents have focused an increasing attention in radiolabelling chemistry over the past decade.[29] The recently reported metal catalysed radiohalogenation of arylboron substrates appeared to us attractive to investigate as it was shown to be efficient at low temperature. However radiolabelling reactions were performed in organic solvents (acetone, methanol, acetonitrile) that are incompatible with antibodies that tolerate only aqueous conditions.[12,30] A recent report on radiobromination showed that a substantial proportion of water (up to 50%) can be tolerated for this reaction although high temperatures were still used (80 °C).[31]

In this study, we aimed to reinvestigate radioiodination and astatination of arylboronic acids in water, at first on a model compound. We then applied the methodology to the ^{125}I-radioiodination and ^{211}At-astatination of an anti-CD138 monoclonal antibody (mAb) that is relevant for targeting multiple myeloma tumour cells. Our novel approach was then compared with the previously reported two-step approach in biodistribution studies with mice grafted with CD138 expressing tumours.

2. Results and discussion

2.1 Preliminary investigation with model compound

Before translation to a relevant biomacromolecule, the reactivity of iodide and astatide with the arylboronic acid functionality in water was probed and optimized with a simple aryl derivative, allowing for accurate analyses by reverse phase radio-HPLC that would not be possible with complex proteins. Thus, 4-chlorobenzeneboronic acid (**1**) was chosen as a model compound for its simplicity. The chloride in *para* position is moderately electron withdrawing (Hammet constant $\sigma = 0.227$) and may be considered as an average substituent in terms of electronic effects that may be found in functionalized compounds. The choice of the substituent, however, does not seem crucial for this preliminary set of experiments as little to no influence of electronic effects on the copper catalyzed radiohalogenation of arylboronic acids or esters was reported (unlike steric effects).[12,30,32]

Before running the radiolabelling in water, we investigated the reaction in organic medium. We started with conditions similar to previous studies that showed Cu(pyridine)$_4$(OTf)$_2$ to be an efficient source of copper(II) for the Chan–Evans–Lam based reaction with radiohalogens.[12,33] The reaction, conducted initially with a relatively high precursor concentration (25 mM) and equimolar amount of catalyst, for 30 min at room temperature, provided nearly quantitative RCYs with both ^{125}I and ^{211}At (Table 1). Interestingly, the same reaction conducted without catalyst led, as expected, to no radioiodination, whereas a substantial RCY (44%) was observed with [^{211}At]NaAt. A nucleophilic process is unlikely to lead to this chemical conversion. Rather, our hypothesis is the possibility for the astatide anion to oxidize in the reaction medium into At^+ that would then react electrophilically with the arylboronic acid

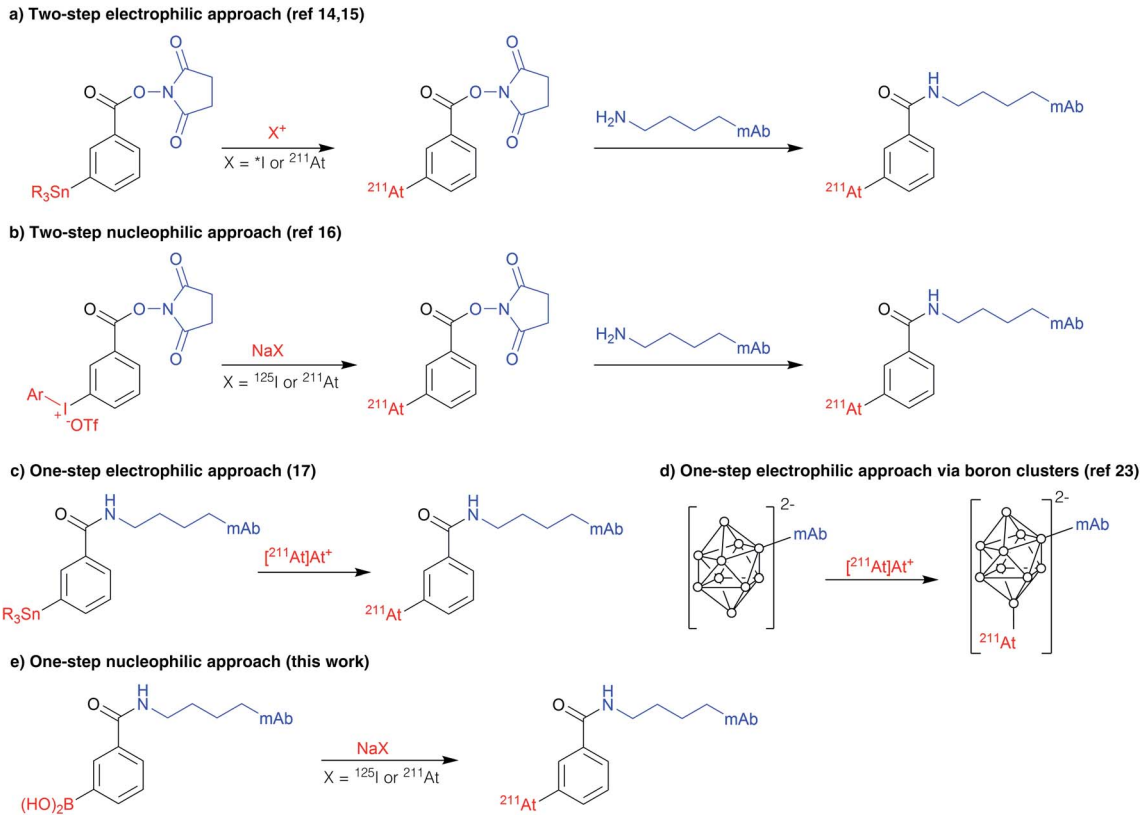

Scheme 1 Strategies for radioiodination and astatination of antibodies.

group. This hypothesis is supported by previous studies having reported on the radioiodination of aryltrifluoroborate or arylboronic acid precursor using electrophilic radioiodide, in the presence or absence of a catalyst.[34,35] We then probed the possibility to reduce the precursor concentration to a level acceptable for mAb radiolabelling. No drop in RCYs was observed when precursor concentration was decrease to 250 μM, a condition being chosen as it corresponds approximately,

Table 1 Preliminary investigation of the ^{125}I-iodination and ^{211}At-astatination of 4-chlorobenzeneboronic acid (**1**). RCYs determined by radio-HPLC analysis of the crude product[a]

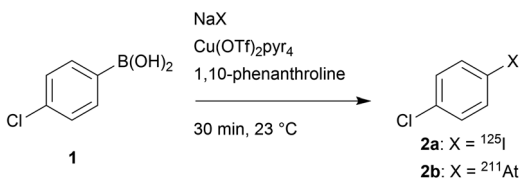

C(**1**) (mM)	C($Cu(OTf)_2pyr_4$) (mM)	C(1,10-phenanthroline) (mM)	Solvent (v : v)	RCY (%)[a] ^{125}I	RCY (%)[a] ^{211}At
25	0	0	MeOH/H_2O (9 : 1)	0	44 ± 7[b]
25	25	0	MeOH/H_2O (9 : 1)	99 ± 1	99 ± 1
10	10	0	MeOH/H_2O (9 : 1)	>99	98 ± 3
0.25	10	0	MeOH/H_2O (9 : 1)	>99	99 ± 1
0.25	10	0	H_2O/MeOH (85 : 15)	17 ± 2	74 ± 5
0.25	0	0	H_2O/MeOH (85 : 15)	—	0
0.25	10	10	H_2O/MeOH (85 : 15)	85 ± 2	>99
0.25	10	10	H_2O/DMF (85 : 15)	91 ± 1	99 ± 1
0.25	10	10	H_2O/DMSO (85 : 15)	88 ± 2	99 ± 1

[a] Standard conditions : [^{125}I]NaI or [^{211}At]NaAt (0.5–1 MBq), 100 μL, 30 min, 23 °C, average of $n = 3$ runs. [b] $n = 7$.

in terms of available arylboronic groups, to a solution of mAb concentrated at 6 mg mL^{-1} with a ratio of 6 arylboronic acids grafted per mAb.

We then switched to aqueous conditions, keeping 15% of methanol as co-solvent for dissolution of the precursor and catalyst. Divergent results were observed for [^{125}I]iodide and [^{211}At]astatide: whereas radioiodination RCY dropped to 17%, it remained at a relatively high level (74%) in the case of astatination. The first hypothesis to explain this difference was an electrophilic pathway with ^{211}At, as in the assay performed in MeOH without catalyst. However, this hypothesis was ruled out as no radiochemical conversion was obtained when the radiolabelling was performed in water without copper salt.

The second hypothesis to explain this large discrepancy is the higher polarizability of astatide, which is consequently less deactivated by hydration than iodide in nucleophilic processes, the nucleophilicity of halogens being increasingly repressed by water from the heaviest to the lightest halogens.

In order to improve RCYs, we added 1,10-phenanthroline to the radiolabelling solution, this kind of ligands having already been reported by Zhang *et al.* and Reilly *et al.* to increase RCYs in organic medium.[12,30] Excellent RCYs were reached again in this case (85% for radioiodination and a quantitative astatination). Radioiodination was further improved by changing methanol to DMF or DMSO to 91% and 88% RCY respectively, whereas astatination RCY remained quantitative. Since DMF was slightly better for radioiodination, and that it is known to be compatible with proteins (when used in reasonable proportions, below 20%), it was kept as a co-solvent for the continued study.

To come closer to radiolabelling conditions compatible with proteins that are generally stored and used in a buffer solution rather than in pure water, we investigated the reaction in relevant buffers (Table 2). All buffers were used at pH 7.4–7.5 in order to dissociate the effect of pH on the reaction from the nature of ions in solution. All tested conditions led to a significant decrease in radioiodination RCY, the worst salt being sodium citrate. This could be explained by chelation of copper(II) by citrates, limiting catalyst availability for the reaction. Chloride ions seem to be disadvantageous for the reaction as RCYs decreased in 0.9% NaCl solution. A hypothesis is the possible competition between chloride ions and iodide or astatide in the reaction. This can also explain in part the poor RCYs observed in PBS, as this solution contains a high concentration of chlorides as well. However, even lower RCYs were observed in PBS compared with NaCl, which may be attributed to the presence of phosphate ions that are known to cause copper precipitation.

Even if no precipitation in PBS was observed in our assays, the interaction between phosphates and the copper catalyst is likely to have altered the reaction. NaCl solution and acetate buffer gave the best results, although moderate RCYs were obtained for radioiodination. However, we observed precipitation of a mAb in these buffers (the 9E7.4 IgG used in radiolabelling assays as discussed below) when the catalyst was added. This precipitation was attributed to the presence of copper(II) in solution since copper salts, and more generally polyvalent metallic ions are known to interact with proteins, leading to their precipitation or degradation.[36,37] Whereas decreasing the copper catalyst or the mAb concentrations were optimizations that could be considered to limit this phenomenon, we choose to investigate the influence of the buffer nature on the protein precipitation. Among the tested buffers, only citrate and Tris prevented precipitation of the proteins. As radioiodination was inefficient in citrate buffer, Tris was selected as the buffer solution to investigate further. It has been previously shown that Tris (tris-(hydroxymethyl)aminomethane) can act as an efficient chelating agent for Cu^{2+} *via* its three hydroxyl groups and its primary amine at pH $\geq$ 7, preventing free copper(II) to interact with proteins.[38] Nonetheless, RCYs were moderate and not satisfying for the development of an efficient radiolabelling method. However, an investigation of the influence of pH showed quantitative RCYs from pH = 7 down to pH = 2 below which the catalyst precipitated (Fig. 1). This last round of optimization showed that arylboronic acid chemistry is extremely efficient for radioiodination and astatination in water and is a realistic approach for the late stage radiolabelling of proteins.

Table 2 Influence of buffer on the ^{125}I-iodination and ^{211}At-astatination of 4-chlorobenzeneboronic acid (**1**). RCYs determined by radio-HPLC analysis of the crude product[a]

Solvent (v : v)	RCY[a] (%)	
	^{125}I	^{211}At
0.9% NaCl/DMF (85 : 15)	38 ± 3	78 ± 13
PBS/DMF (85 : 15)	21 ± 2	31 ± 7
Sodium acetate buffer 0.1 M pH 7.5/DMF (85 : 15)	40 ± 4	84 ± 8
Sodium citrate buffer 0.5 M pH 7.5/DMF (85 : 15)	0[b]	—
Tris buffer 0.5 M pH 7.5/DMF (85 : 15)	35 ± 8	47 ± 9

[a] Standard conditions: (**1**) (0.25 mM), $Cu(OTf)_2pyr_4$ (10 mM), 1,10-phenanthroline (10 mM), [^{125}I]NaI or [^{211}At]NaAt (1–5 MBq), 30 min, 100 µL, 23 °C, n = 3. [b] $Cu(OTf)_2pyr_4$ (5 mM), 1,10-phenanthroline (5 mM).

2.2 Arylboronic acid conjugation to mAb and radiolabelling

In order to investigate the potential of this chemical approach on a relevant cancer targeting mAb, we chose the 9E7.4 mAb.

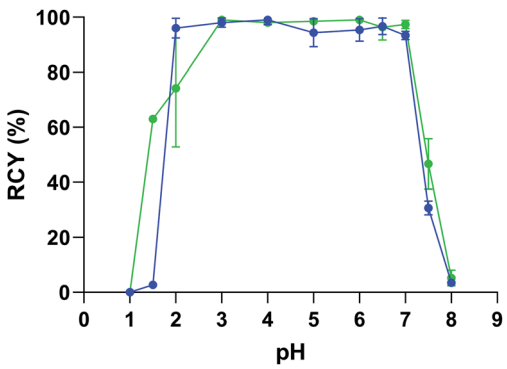

Fig. 1 Influence of pH on the ^{125}I-iodination (●) and ^{211}At-astatination (●) of 4-chlorobenzeneboronic acid (**1**). RCYs determined by radio-HPLC analysis of the crude product. Standard conditions: (**1**) (0.25 mM), $Cu(OTf)_2pyr_4$ (10 mM), 1,10-phenanthroline (10 mM), [^{125}I]NaI or [^{211}At]NaAt (1–5 MBq), Tris buffer 0.5 M/DMF (85:15), 30 min, 100 µL, 23 °C, $n \geq 2$.

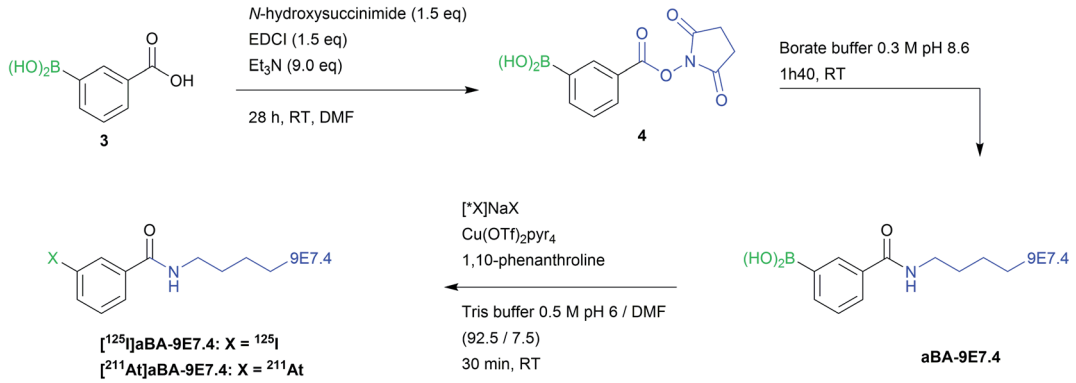

Scheme 2 Strategy for late stage ^{125}I-iodination and ^{211}At-astatination of 9E7.4 mAb *via* arylboronic acid chemistry.

This rat anti-mouse CD138 antibody developed in our laboratory has previously shown suitable properties for the study of targeted alpha therapy, including with ^{211}At, or beta therapy and immunoPET imaging of multiple myeloma in a syngeneic animal model.[39–42]

Bioconjugation of arylboronic acid groups with the 9E7.4 mAb was performed on amino groups of the lysine residues using 3-(succinimidyloxycarbonyl)phenylboronic acid (**4**) prepared from 3-boronobenzoic acid, providing aBA-9E7.4 (Scheme 2). Precursor (**4**) was chosen as it leads to the same radiolabelled mAbs than with the widely used two-step approach based on the conjugation of SIB or SAB to lysine groups, allowing direct comparison of methods. When 10 equivalents of (**4**) were used in the coupling step, we measured a ratio of 3.4 ± 0.6 arylboronic acid groups/mAb by mass spectrometry (see ESI Fig. S7†), a value that we considered as sufficient to perform radiolabelling while being low enough to expect preservation of protein pharmacokinetic properties.

First radiolabelling assays performed on aBA-9E7.4 using optimal conditions defined with the model compound (Tris buffer pH 6, with a reduction of the DMF ratio to 7.5% instead of 15% in order to lower the risk of protein denaturation), provided excellent results, with RCYs of 87 ± 1% and 94 ± 3% for ^{125}I-iodination and ^{211}At-astatination, respectively. In order to limit the risk of protein alteration or the presence of residual copper in the final radiopharmaceutical, we investigated further the possibility to reduce the catalyst concentration during the radiolabelling step, while keeping an equimolar amount of ligand. Radioiodination RCYs were observed to decrease steadily (from 87% to 58%) while catalyst concentration was decreased from 10 mM to 1.25 mM (Table 3). On the other hand, astatination RCYs remained unchanged (93–96%) even at the lowest concentration tested.

We then investigated the non-specific binding of ^{125}I and ^{211}At to the mAb. For this, the unmodified mAb (not conjugated with the arylboronic acid precursor (**4**)) was submitted to the same radiolabelling conditions. In the case of radioiodination, non-specific binding to 9E7.4 was insignificant (≤1.2%) whereas astatination was high (62 ± 8% with 10 mM catalyst and ligand). ^{211}At binding was reduced by half when using 5 mM catalyst and ligand concentration, but it could not be further reduced at lower concentrations. The binding of astatine on proteins is an already known phenomenon as discussed below. Since radioiodination RCY remained satisfyingly

Table 3 Influence of catalyst and ligand concentration on radioiodination and astatination RCY of 9E7.4-aBA[a]

	RCY (%)			
	^{125}I		^{211}At	
Catalyst and ligand concentration (mM)	9E7.4-aBA	9E7.4	9E7.4-aBA	9E7.4
10	87 ± 1	0.4	94 ± 3	62 ± 8
5	79 ± 4	1.2	93 ± 4	42 ± 5
2.5	73 ± 2	—	96 ± 1	32 ± 7
1.25	58 ± 8	0.3	93 ± 4	37 ± 12

[a] Standard conditions: modified 9E7.4-aBA or unmodified 9E7.4 (32 μM), $Cu(OTf)_2Pyr_4$, 1,10-phenanthroline, [^{125}I]NaI or [^{211}At]NaAt (1–5 MBq), 30 min, 23 °C in 0.5 M TRIS buffer/DMF (92.5 : 7.5), $n \geq 3$. RCYs are based on the radio-TLC analysis of the crude product.

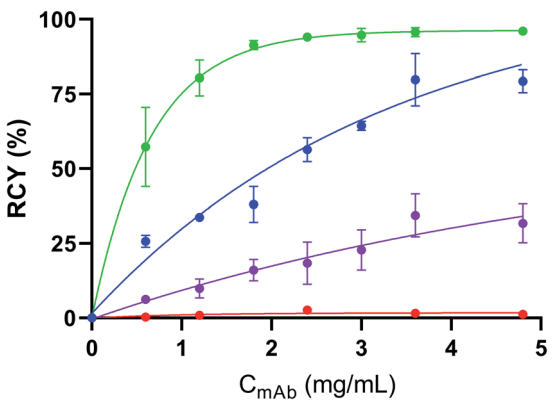

Fig. 2 Influence of mAb concentration on the ^{125}I-radioiodination[a] of aBA-9E7.4 (•) and 9E7.4 (•) and ^{211}At-astatination[b] of aBA-9E7.4 (•) and 9E7.4 (•). RCYs determined by radio-ITLC-SG analysis of the crude product. Standard conditions: 30 min, 100 μL, 23 °C, Tris buffer 0.5 M pH 6/DMF (92.5 : 7.5), $n \geq 2$. [a] $Cu(OTf)_2pyr_4$ (5 mM), 1,10-phenanthroline (5 mM), [^{125}I]NaI (1–5 MBq) [b] $Cu(OTf)_2pyr_4$ (2.5 mM), 1,10-phenanthroline (2.5 mM), [^{211}At]NaAt (1–5 MBq).

Table 4 Comparison between the two-step approaches *via* electrophilic or nucleophilic pathway and the arylboronic acid method for the ^{125}I-iodination and ^{211}At-astatination of the 9E7.4 mAb

Method	RCYs (%)		Activity yield[c] (MBq)		Specific activity[c] (MBq mg^{-1})		Duration time (min)
	^{125}I	^{211}At	^{125}I	^{211}At	^{125}I	^{211}At	
Two-step electrophilic[a]	—	20–30	—	5.5	—	24.4	200 ± 10
Two-step nucleophilic[b]	43	53–57	12.9	13.2	57.3	58.7	140 ± 10
This work	80	56–68	24	16.1	66.7	119	90 ± 10

[a] [^{211}At]SAB prepared from the tin precursor with *N*-chlorosuccinimide as oxidizing agent before the conjugation to the mAb ($n = 2$). [b] [^{125}I]SIB or [^{211}At]SAB prepared from the aryliodonium salt with sodium sulfite as reducing agent before conjugation to the mAb ($n = 5$). [c] Starting with 30 MBq.

elevated (79 ± 4%) with 5 mM catalyst and ligand concentration, we selected this concentration for the rest of this study whereas it was set at 2.5 mM for astatination.

We then investigated the influence of the mAb concentration on the RCYs, the purposes being: (i) to probe the possibility to reduce ^{211}At non-specific binding on the mAb and (ii) to optimize the specific activity (A_s) that can be achieved by this method. Initial conditions discussed above used the mAb at a concentration of 4.8 mg mL^{-1}, which is the minimum needed for efficient radioiodination or astatination of this mAb by two-step approaches. This concentration may vary depending on mAbs.[49] This relatively elevated concentration limits optimization of A_s. Radioiodination RCYs remained optimal (80 ± 9%) when aBA-9E7.4 concentration was decreased to 3.6 mg mL^{-1} (Fig. 2), and decreased progressively along with further concentration decrease. In the case of astatination, the mAb concentration could be further reduced to 1.8 mg mL^{-1} without significantly impacting the RCY (91 ± 2% *vs.* 96 ± 1% at the highest tested concentrations). Interestingly, non-specific binding of ^{211}At on 9E7.4 also decreased with mAb concentration from 32 ± 7% at 4.8 mg mL^{-1} to 16 ± 4% at 1.8 mg mL^{-1} or even 6 ± 1% at 0.6 mg mL^{-1}.

It is known that free astatine can bind to proteins as reported in previous studies. In particular At(I) species have been shown to bind weakly to proteins in the absence of free sulfhydryl group from cysteine at their surface. The bond formed is so weak that At dissociates extensively upon protein precipitation or when the protein is passed through a Sephadex gel during chromatographic analysis or purification.[22] From results depicted in Fig. 2, the possibility that non-specific binding occurs competitively with expected astatodeboronation reaction was investigated. For this, we performed a size exclusion chromatographic purification (using a Sephadex based PD10 column) of both astatinated aBA-9E7.4 and unmodified 9E7.4 followed by a chromatographic analysis on ITLC-SG strips using MeOH as eluent of the purified products. Under these conditions, proteins precipitate at the deposit point whereas free astatine migrates with the solvent front. Chromatographic analyses showed that, after purification, activity was detected all along the ITLC-SG strip in the case of the unmodified [^{211}At]9E7.4 due to the progressive release of weakly bound astatine from the mAb during the elution (Fig. S6†). Conversely, the radiochemical purity of [^{211}At]aBA-9E7.4 was very high, most of the activity remaining at the bottom of the TLC (>99%). These results suggest that non-specific binding does not occur during ^{211}At-astatination of the aBA-9E7.4, or that if occurring, it is removed during the purification step.

The similar chromatographic and precipitation behaviour of non-specifically astatinated 9E7.4 suggests a similar mode of weak binding than previously reported by Visser *et al.*[22] The nature of this bond was recently reinvestigated by molecular modelling, suggesting the formation of covalent bonds between the AtO^+ species and nitrogen and sulphur atoms on proteins.[43]

In order to investigate the potential impact of this approach in a pre-clinical research setting, we performed radioiodination and astatination of the mAb with the optimized conditions, at higher activities (≈30 MBq starting activity). Results were compared with the classical two-step approaches *via* electrophilic and nucleophilic labelling reported previously for this mAb.[16] Our method led to significantly improved results regarding major aspects (Table 4): RCYs, activity yields and specific activities (due to the lower amount of mAb needed) were increased whereas the procedure time was decreased. The time aspect is of high importance with radionuclides with short half-life such as ^{211}At. As the use of a copper catalyst can be a problem related to copper toxicity, we investigated the

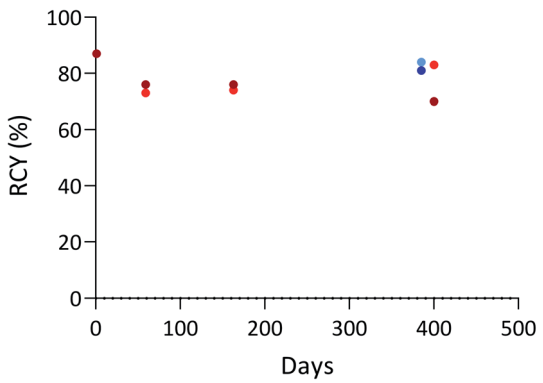

Fig. 3 Radiolabelling of aBA-9E7.4 with ^{125}I after storage at 4 °C (●) or −18 °C (●)[a] and ^{211}At after storage at 4 °C (●) or −18 °C (●)[b] in Tris buffer 0.5 M at pH 6. Standard conditions: 30 min, 100 µL, 23 °C. [a] $Cu(OTf)_2pyr_4$ (5 mM), 1,10-phenanthroline (5 mM), [^{125}I]NaI (1–10 MBq) [b] $Cu(OTf)_2pyr_4$ (2.5 mM), 1,10-phenanthroline (2.5 mM), Tris buffer 0.5 M pH 6/DMF (92.5 : 7.5), [^{211}At]NaAt (1–5 MBq). RCYs determined by radio-ITLC-SG analysis of the crude product.

presence of residual Cu by Induced Coupled Plasma-Mass Spectrometry (ICP-MS) of the purified astatinated aBA-9E7.4. Results showed that the copper concentration was below the detection limit of 1 ppm.

2.3 Immunoreactivity and precursor shelf-life

The immunoreactivity, which illustrates the proportion of protein in a batch that is able to bind to its target, was measured for both ^{125}I-iodinated and ^{211}At-astatinated 9E7.4. Immunoreactive fraction (IRF) of 90% and 88% were respectively obtained with ^{125}I- and ^{211}At-labelled 9E7.4. These results were similar to the unmodified 9E7.4 (IRF = 85%) or to the previously reported two-step labelling procedure (IRF = 86% for ^{125}I-iodination and ^{211}At-astatination),[16] indicating an excellent preservation of the mAb.

In addition, to check that the aBA-9E7.4 immunoconjugate can be stored in solution and used over time, we performed a series of radiolabelling assays with the same production batch stored in the radiolabelling buffer (Tris buffer at pH = 6) either at 4 °C or – 18 °C over more than a year (Fig. 3). High RCYs were maintained during the whole study (close to 80% with both radionuclides), which indicates that protodeboronation that may impact boronic acid compounds in water as reported previously does not occur significantly under investigated storage conditions.[44,45] The integrity of the mAb was also verified *via* its immunoreactivity and IRFs of 85% and 90% for the conjugate stored at 4 °C and −18 °C were respectively measured after radioiodination, confirming that it was not altered by the storage conditions. These results suggest the possibility to develop storable radiolabelling kits containing the pre-modified mAb and the reagents needed, facilitating the production of labelled antibodies in a clinical setting.

2.4 Biodistribution study

To confirm the viability of this technology for *in vivo* applications, biodistribution of both ^{125}I-iodinated and ^{211}At-astatinated aBA-9E7.4 was monitored over 21 h after intravenous injection on BALB/c mice grafted subcutaneously with the CD138 expressing MOPC-315 plasmacytoma cell line. Results were compared with the conventional two-step approach that consisted in the synthesis of [^{125}I]SIB and [^{211}At]SAB intermediates followed by conjugation to the mAb.[16]

Overall, biodistribution data indicated that the pharmacokinetic profiles were globally preserved when using our single-step approach since % ID g^{-1} values were nearly identical ($p > 0.05$) for most major organs when comparing both radioiodination approaches (Fig. 4A and B) or both astatination approaches (Fig. 5A and B). For ^{125}I-labelling, significant

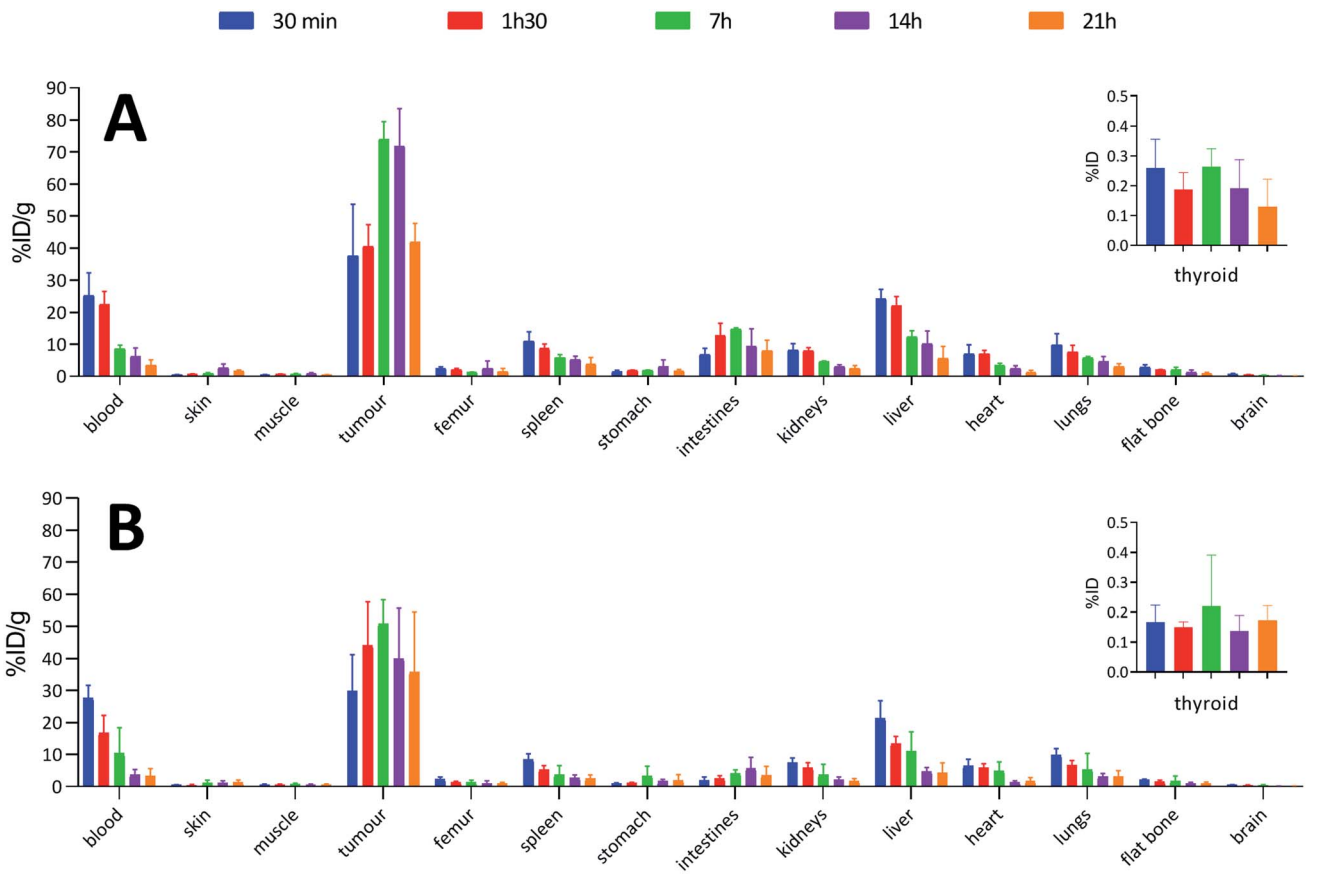

Fig. 4 Biodistributions in BALB/c mice with subcutaneous tumours (MOPC-315) injected with: (A) 0.04 MBq of ^{125}I-labelled 9E7.4 *via* the two-step method; (B) 0.04 MBq of ^{125}I-labelled 9E7.4 *via* the arylboronic acid single-step method.

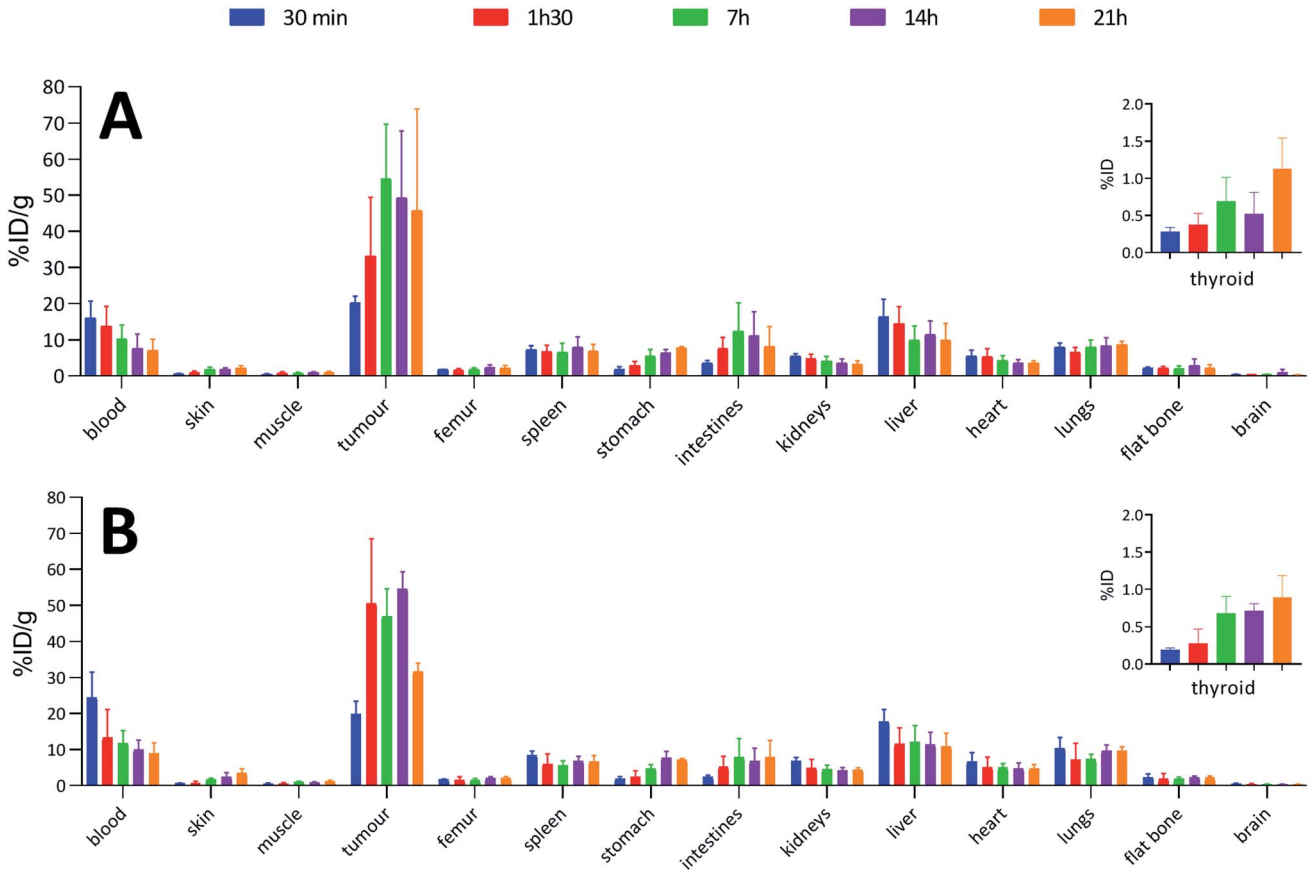

Fig. 5 Biodistributions in BALB/c mice with subcutaneous tumours (MOPC-315) injected with: (A) 1 MBq of ^{211}At-labelled 9E7.4 *via* the two-step method; (B) 1 MBq of ^{211}At-labelled 9E7.4 *via* the arylboronic acid single-step method.

differences between both methods appeared in intestines at 1 h 30 ($p = 0.0080$) and 7 h ($p = 0.0009$) and in the liver at 1 h 30 ($p = 0.0348$) for which a significantly reduced uptake was visible using the single-step labelling approach. The only statistical difference with the astatination was for blood at 30 min ($p = 0.0006$), which was lower using the two-step approach.

In all cases, high uptake was observed in tumours. The significantly higher tumour uptake observed with the two-step ^{125}I-labelling at 7 h ($p < 0.0001$) and 14 h ($p < 0.0001$) and with the one-step ^{211}At-labelling at 1 h 30 ($p = 0.0003$) can be explained by the lower tumour weight of the mice in these groups. Indeed, radioimmunoconjugate uptake in the tumour appeared to be inversely correlated to the tumour weight (Fig. 6), which may be explained by the difference in vasculature between large and small tumours (unpublished observation). Large tumours are often poorly vascularized with high interstitial pressure leading to the development of necrotic tissues in their centre with a loss of CD138 expression.

When comparing radioiodinated 9E7.4 with the astatinated analogue within the same radiolabelling strategy, both led to the same higher uptake in thyroid, stomach, spleen, lungs and kidneys with the ^{211}At-immunoconjugates. This observation was expected and can be attributed to the progressive release of ^{211}At from the carrier IgG *in vivo* since these organs are well-known targets of free astatine.[46] The instability remained however moderate, with a relatively slow increase of uptake over time in these organs, and it was not impacted by the radiolabelling method employed ($p > 0.05$). Research for novel labelling strategies involving other bonds than aryl–astatine bonds with improved stability remains one of the biggest challenges, with a pressing need especially for applications with small, rapidly metabolized carrier compounds. In our case, the

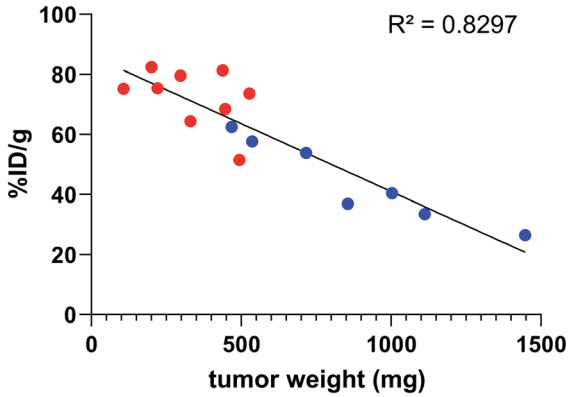

Fig. 6 Activity uptake in tumour compared to tumour weight 7 h and 14 h post injection of 9E7.4 ^{125}I-iodinated by the two-step method (•) or the arylboronic acid single-step method (•).

instability remained moderate, and if needed, this non-specific uptake may be reduced significantly by the use of appropriate blocking agents.[47] We decided to not use them in our experiment to check the presence of free ^{211}At, or ^{211}At weakly bound to the IgG in the injected solution, which would rapidly result in a higher uptake in thyroid at early biodistribution points. Our results indicated a low ^{211}At uptake in thyroid in the shortest time (<0.3% ID at 0.5 h), similarly to iodine, followed by a progressive increase in uptake with a difference visible only after 7 h. Consequently, the analysis of thyroid activity uptake excludes the hypothesis of residual non-specifically bound astatine discussed in previous sections, as it would have resulted in a rapid increase in activity uptake in this tissue.

3. Conclusions

We demonstrated herein the high reactivity of arylboronic acids with radioiodide and astatide in water at room temperature, suggesting their high potential for radiolabelling sensitive carrier bio(macro)molecules. The standard conditions set up on a simple model compound were straightforwardly translated to the radiolabelling of an anti-CD138 mAb relevant for the imaging and treatment of multiple myeloma. We showed that the new procedure, based on a nucleophilic single-step approach, outperformed previously reported methods in terms of RCYs, activity yields, specific activities and duration, while maintaining nearly identical radioimmunoconjugates biodistribution and high uptake on CD138 expressing tumours in mice. The first divergent radiosynthesis of a radioiodinated mAb and its ^{211}At-labelled analogue, performed in a single step from a common pre-conjugated aryl precursor was reported, facilitating perspectives for radiotheranostic applications using radioiodide/^{211}At pairs. Additionally, the long-term stability in solution of the mAb pre-modified by conjugation with arylboronic acids led to high RCYs over more than a year, suggesting the possibility to develop ready-to-use radiolabelling kits. Overall, the efficiency and simplification provided by this novel approach should facilitate the transfer of astatinated radiopharmaceuticals and their theranostic combinations into the clinic.

4. Experimental section

4.1 Radiochemistry

4.1.1. General. [^{125}I]NaI was obtained commercially from PerkinElmer in 10^{-5} M NaOH solution with a volumic activity of 1.85 MBq μL^{-1} (50 μCi μL^{-1}). ^{211}At was produced at the Arronax cyclotron facility using the ^{209}Bi(α,2n)^{211}At reaction and recovered from the irradiated target in chloroform using a dry-distillation protocol adapted from the procedure previously reported by Lindegren *et al.*[48] [^{211}At]NaAt was then obtained by reducing to dryness the chloroformic astatine solution under a gentle stream of nitrogen to obtain dry astatine, followed by dissolution with an aqueous sodium sulfite solution. HPLC analyses were performed on a Waters Alliance e2695 system equipped with a FlowStar LB 513 Radio Flow Detector and a C-18 column (Spherisorb ODS2 5μ 4.6 mm × 25 cm, Waters) with the flow rate set at 1.50 mL min^{-1} with the following gradient: t = 0: 60% A, 40% B; t = 7 min: 30% A, 70% B; t = 11 min: 100% B with A = H_2O with 0.05% TFA and B = CH_3CN with 0.05% TFA. After each HPLC analysis, the column was washed by injection of a 10 mg mL^{-1} sodium sulfite solution (50 μL) with the following gradient: t = 0: 100% A, 0% B; t = 5 min, 60% A, 40% B. The activity released during this run, which corresponded to free radionuclide bound to the column material, was taken into account for the calculation of RCYs of the preceding run. The non-radioactive iodinated compounds were analysed using this HPLC system and their retention times were used as references for identification of their radioiodinated and astatinated analogues (see ESI Fig. S3–S5† for representatives examples).

4.1.2. ^{125}I-iodination and ^{211}At-astatination of 4-chlorobenzeneboronic acid 1 in organic medium. Stock solutions of [^{125}I]NaI were prepared by diluting the commercial solution in de-ionized water. Stock solution of [^{211}At]NaAt were prepared by adding an appropriate volume of a 1 mg mL^{-1} sodium sulfite solution on the dry ^{211}At residue. 70 μL of MeOH, 10 μL of **1** (2.5 mM) in MeOH and 10 μL of Cu(OTf)$_2$pyr$_4$ (100 mM) in MeOH were placed in a 1.5 mL HPLC vial, and 10 μL of the stock solution of [^{125}I]NaI or [^{211}At]NaAt were added (≈0.5 MBq). The vial was then stirred vigorously at room temperature for 30 min. An aliquot was then diluted in a solution of CH_3CN/water 1 : 1 (0.05% TFA) and analysed by reverse phase HPLC.

4.1.3. ^{125}I-iodination and ^{211}At-astatination of 4-chlorobenzeneboronic acid 1 in aqueous medium. 75 μL of 0.5 M Tris buffer pH 6, 3 μL of **1** (8.33 mM) in DMF, 8 μL of Cu(OTf)$_2$pyr$_4$ (125 mM) in DMF and 4 μL of 1,10-phenanthroline (250 mM) in DMF were placed in a 1.5 mL vial, and 10 μL of the stock solution of [^{125}I]NaI or [^{211}At]NaAt were added. The vial was then stirred vigorously at room temperature for 30 min. An aliquot was then diluted in a solution of CH_3CN/water 1/1 (0.05% TFA) and analysed by reverse phase HPLC.

4.2 Protein radiolabeling

4.2.1 Bioconjugation of arylboronic acid 4. To a 5 mg mL^{-1} solution of anti-CD138 mAb in 0.3 M borate buffer (pH 8.6, 1.4 mL) were added 10 equivalents of **4** (preparation reported in ESI) in DMSO (25 μL). The solution was stirred at room temperature for 100 min upon which the unconjugated acid was removed by ultracentrifugation with 30 K centrifugal filters (Merck) using the buffer needed for radiolabeling.

4.2.2. ^{125}I-iodination of aBA-9E7.4. To aBA-anti-CD138 in 0.5 M TRIS buffer at pH = 6.0 at a concentration of 4.5 mg mL^{-1} (80 μL) were added a solution of 100 mM Cu(OTf)$_2$pyr$_4$ in 0.5 M TRIS buffer pH 6/DMF (1 : 1) (5 μL), 100 mM 1.10-phenanthroline in DMF (5 μL), and [^{125}I]NaI (10 μL, 1 to 33 MBq). After 30 min of incubation at room temperature, RCY was assessed by elution of an aliquot deposited on an ITLC-SG strip (MeOH as eluent), and analysis of the strip using a Cyclone phosphor-imager scanner (PerkinElmer). Purification was performed by gel filtration on a Sephadex G-25 resin loaded column (PD-10, GE healthcare) using PBS as eluent, affording the purified radiolabelled antibody (**6a**) with a >99% radiochemical purity as assessed by ITLC-SG.

4.2.3. ^{211}At-astatination of aBA-9E7.4. A stock solution of [^{211}At]NaAt was prepared by addition of an appropriate volume of a 0.0625 mg mL^{-1} sodium sulfite solution to dry ^{211}At. To aBA-9E7.4 in 0.5 M Tris buffer (pH = 6.0) concentrated at 2.25 mg mL^{-1} (80 μL) were added Cu(OTf)$_2$pyr$_4$ in 0.5 M TRIS buffer pH 6/DMF (1 : 1) (50 mM, 5 μL), 1.10-phenanthroline in DMF (50 mM, 5 μL), and [^{211}At]NaAt (10 μL, 1 to 40 MBq). After 30 min of incubation at room temperature, RCY was assessed by ITLC-SG strip similarly to radioiodination. Purification was performed by gel filtration on a Sephadex G-25 resin loaded column (PD-10, GE healthcare) using PBS as eluent, affording the purified radiolabelled antibody (**6b**) with a >99% radiochemical purity as assessed by ITLC-SG.

4.2.4. Immunoreactivity assays. The immunoreactive fractions (IRFs) of [^{125}I]aBA-9E7.4 and [^{211}At]aBA-9E7.4 were determined using magnetic beads (Pierce, Thermo Scientific) conjugated with a 40 amino acids peptide produced by Genecust which is recognized by the anti-CD138 antibody according to the supplier's protocol. 0.1 picomole of radiolabeled aBA-9E7.4 was incubated for 15 min at room temperature with 10 μL of coated magnetic beads (10 mg mL^{-1}). Using a magnetic rack, supernatants containing non-reactive antibodies and magnetic beads were collected separately and the radioactivity in each fraction was measured in a gamma counter.

4.3. *In vivo* studies

4.3.1. Biodistribution studies. Female BALB/c mice were purchased from Janvier Labs and housed under conventional conditions at the Experimental Therapeutic Unit animal facility (SFR François Bonamy, IRS-UN, Nantes University, license number: B-44-278). Mice were 8 weeks old at the time of experiment. Experiment was approved by the local veterinary committee (APAFIS #6145).

BALB/c mice were inoculated subcutaneously with 2×10^5 MOPC-315 plasmacytoma cells (ATCC® TIB-23™). When tumour size was between 200 and 1500 mm^3, the animals were divided in 4 groups. Group A was treated with [^{125}I]aBA-9E7.4 (40 kBq per mice, 20 μg in 100 μL), group B with [^{125}I]9E7.4 radiolabelled *via* the two-step method (40 kBq per mice, 20 μg in 100 μL), group C with [^{211}At]aBA-9E7.4 (1 MBq per mice, 20 μg in 100 μL), and group D with [^{211}At]9E7.4 radiolabelled *via* the two-step method (1 MBq per mice, 20 μg in 100 μL).[16] The mice were sacrificed by cervical dislocation in groups of 3 to 6 animals at 5 different time points post injection: 30 min, 1 h 30, 7 h, 14 h and 21 h. The selected tissues (blood, skin, muscle, tumour, femur, spleen, stomach, intestines, kidneys, liver, heart, lungs, flat bone, brain) were dissected, weighed and counted on a calibrated and normalized gamma-counter (PerkinElmer). For each organ, the percentage of injected dose per gram (% ID g^{-1}) was calculated. The neck (thyroid) was not weighed but counted as well on the gamma counter for the determination of the % ID. No blocking agent were used in order to use organs uptake (thyroid, stomach, spleen, lungs, kidneys, liver) as indicator of free astatine.

4.3.2. Statistical analysis. Statistical analysis was performed using GraphPad Prism version 8.00. Differences in organ uptake were tested for significance using the Sidak's multiple comparison test. A p value below 0.05 was considered significant.

Conflicts of interest

The authors declare the following competing financial interest: M. B., A. F.-C., J.-F. G. and F. G. have filed a provisional patent application relating to this work.

Acknowledgements

This work was supported by grants from the French National Agency for Research called "Investissements d'Avenir", Equipex Arronax-Plus (ANR-11-EQPX-0004), Labex IRON (ANR-11-LABX-18-01), ISITE NExT (ANR-16-IDEX-0007) and INCa-DGOS-Inserm_12558. The UTE facility (SFR Santé) and the radioactivity platform (SFR Santé) are thanked for the technical assistance.

Notes and references

1 M. Makvandi, E. Dupis, J. W. Engle, F. M. Nortier, M. E. Fassbender, S. Simon, E. R. Birnbaum, R. W. Atcher, K. D. John, O. Rixe and J. P. Norenberg, *Target. Oncol.*, 2018, **13**, 189–203.
2 C. Parker, V. Lewington, N. Shore, C. Kratochwil, M. Levy, O. Lindén, W. Noordzij, J. Park and F. Saad, *JAMA Oncol.*, 2018, **4**, 1765–1772.
3 F. Guérard, J.-F. Gestin and M. W. Brechbiel, *Cancer Biother.Radiopharm.*, 2013, **28**, 1–20.
4 M. R. Zalutsky, D. A. Reardon, G. Akabani, R. E. Coleman, A. H. Friedman, H. S. Friedman, R. E. McLendon, T. Z. Wong and D. D. Bigner, *J. Nucl. Med.*, 2008, **49**, 30–38.
5 H. Andersson, E. Cederkrantz, T. Bäck, C. Divgi, J. Elgqvist, J. Himmelman, G. Horvath, L. Jacobsson, H. Jensen, S. Lindegren, S. Palm and R. Hultborn, *J. Nucl. Med.*, 2009, **50**, 1153–1160.
6 S. O'Steen, M. L. Comstock, J. J. Orozco, D. K. Hamlin, D. S. Wilbur, J. C. Jones, A. Kenoyer, M. E. Nartea, Y. Lin, B. W. Miller, T. A. Gooley, S. A. Tuazon, B. G. Till, A. K. Gopal, B. M. Sandmaier, O. W. Press and D. J. Green, *Blood*, 2019, **134**, 1247–1256.
7 T. Ferris, L. Carroll, S. Jenner and E. O. Aboagye, *J. Labelled Compd. Radiopharm.*, DOI: 10.1002/jlcr.3891.
8 M. J. Adam and D. S. Wilbur, *Chem. Soc. Rev.*, 2005, **34**, 153–163.
9 L. Xie, M. Hanyu, M. Fujinaga, Y. Zhang, K. Hu, K. Minegishi, C. Jiang, F. Kurosawa, Y. Morokoshi, H. K. Li, S. Hasegawa, K. Nagatsu and M.-R. Zhang, *J. Nucl. Med.*, 2020, **61**, 242–248.
10 F. Guérard, Y.-S. Lee, K. Baidoo, J.-F. Gestin and M. W. Brechbiel, *Chem.–Eur. J.*, 2016, **22**, 12332–12339.
11 L. Navarro, M. Berdal, M. Chérel, F. Pecorari, J.-F. Gestin and F. Guérard, *Bioorg. Med. Chem.*, 2019, **27**, 167–174.
12 S. W. Reilly, M. Makvandi, K. Xu and R. H. Mach, *Org. Lett.*, 2018, **20**, 1752–1755.
13 D.-C. Sergentu, D. Teze, A. Sabatié-Gogova, C. Alliot, N. Guo, F. Bassal, I. D. Silva, D. Deniaud, R. Maurice, J. Champion,

N. Galland and G. Montavon, *Chem.–Eur. J.*, 2016, **22**, 2964–2971.
14 M. R. Zalutsky, P. K. Garg, H. S. Friedman and D. D. Bigner, *Proc. Natl. Acad. Sci. U. S. A.*, 1989, **86**, 7149–7153.
15 M. R. Zalutsky and A. S. Narula, *Int. J. Radiat. Appl. Instrum., Part A*, 1987, **38**, 1051–1055.
16 F. Guérard, L. Navarro, Y.-S. Lee, A. Roumesy, C. Alliot, M. Chérel, M. W. Brechbiel and J.-F. Gestin, *Bioorg. Med. Chem.*, 2017, **25**, 5975–5980.
17 S. Lindegren, S. Frost, T. Bäck, E. Haglund, J. Elgqvist and H. Jensen, *J. Nucl. Med.*, 2008, **49**, 1537–1545.
18 E. Aneheim, A. Gustafsson, P. Albertsson, T. Bäck, H. Jensen, S. Palm, S. Svedhem and S. Lindegren, *Bioconjugate Chem.*, 2016, **27**, 688–697.
19 D. S. Wilbur, S. W. Hadley, M. D. Hylarides, P. G. Abrams, P. A. Beaumier, A. C. Morgan, J. M. Reno and A. R. Fritzberg, *J. Nucl. Med.*, 1989, **30**, 216–226.
20 G. W. M. Visser, E. L. Diemer and F. M. Kaspersen, *Int. J. Appl. Radiat. Isot.*, 1979, **30**, 749–752.
21 G. W. M. Visser, E. L. Diemer and F. M. Kaspersen, *Int. J. Appl. Radiat. Isot.*, 1980, **31**, 275–278.
22 G. W. M. Visser, E. L. Diemer and F. M. Kaspersen, *Int. J. Appl. Radiat. Isot.*, 1981, **32**, 905–912.
23 D. S. Wilbur, M.-K. Chyan, D. K. Hamlin and M. A. Perry, *Nucl. Med. Biol.*, 2010, **37**, 167.
24 K. Fujiki, Y. Kanayama, S. Yano, N. Sato, T. Yokokita, P. Ahmadi, Y. Watanabe, H. Haba and K. Tanaka, *Chem. Sci.*, 2019, **10**, 1936–1944.
25 H. Jadvar, X. Chen, W. Cai and U. Mahmood, *Radiology*, 2018, **286**, 388–400.
26 K. Ogawa, T. Takeda, K. Mishiro, A. Toyoshima, K. Shiba, T. Yoshimura, A. Shinohara, S. Kinuya and A. Odani, *ACS Omega*, 2019, **4**, 4584–4591.
27 G. J. Meyer, K. Roessler and G. Stoecklin, *J. Am. Chem. Soc.*, 1979, **101**, 3121–3123.
28 G. J. Meyer, A. Walte, S. R. Sriyapureddy, M. Grote, D. Krull, Z. Korkmaz and W. H. Knapp, *Appl. Radiat. Isot.*, 2010, **68**, 1060–1065.
29 T. C. Wilson, T. Cailly and V. Gouverneur, *Chem. Soc. Rev.*, 2018, **47**, 6990–7005.
30 P. Zhang, R. Zhuang, Z. Guo, X. Su, X. Chen and X. Zhang, *Chem.–Eur. J.*, 2016, **22**, 16783–16786.
31 D. Zhou, W. Chu, T. Voller and J. A. Katzenellenbogen, *Tetrahedron Lett.*, 2018, **59**, 1963–1967.
32 T. C. Wilson, G. McSweeney, S. Preshlock, S. Verhoog, M. Tredwell, T. Cailly and V. Gouverneur, *Chem. Commun.*, 2016, **52**, 13277–13280.
33 M. Tredwell, S. M. Preshlock, N. J. Taylor, S. Gruber, M. Huiban, J. Passchier, J. Mercier, C. Génicot and V. Gouverneur, *Angew. Chem., Int. Ed.*, 2014, **53**, 7751–7755.
34 G. W. Kabalka and M.-L. Yao, *J. Organomet. Chem.*, 2009, **694**, 1638–1641.
35 S. Webster, K. M. O'Rourke, C. Fletcher, S. L. Pimlott, A. Sutherland and A.-L. Lee, *Chem.–Eur. J.*, 2018, **24**, 937–943.
36 M. V. Dam, G. E. Wuenschell and F. H. Arnold, *Biotechnol. Appl. Biochem.*, 1989, **11**, 492–502.
37 Z. K. Glover, L. Basa, B. Moore, J. S. Laurence and A. Sreedhara, *mAbs*, 2015, **7**, 901–911.
38 J. Nagaj, K. Stokowa-Soltys, E. Kurowska, T. Frączyk, M. Jeżowska-Bojczuk and W. Bal, *Inorg. Chem.*, 2013, **52**, 13927–13933.
39 N. Fichou, S. Gouard, C. Maurel, J. Barbet, L. Ferrer, A. Morgenstern, F. Bruchertseifer, A. Faivre-Chauvet, E. Bigot-Corbel, F. Davodeau, J. Gaschet and M. Chérel, *Front. Med.*, 2015, **2**, 76.
40 C. Bailly, S. Gouard, M. Lacombe, P. Remaud-Le Saëc, B. Chalopin, M. Bourgeois, N. Chouin, R. Tripier, Z. Halime, F. Haddad, A. Faivre-Chauvet, F. Kraeber-Bodéré, M. Chérel and C. Bodet-Milin, *Oncotarget*, 2018, **9**, 9061–9072.
41 C. Bailly, S. Gouard, F. Guérard, B. Chalopin, T. Carlier, A. Faivre-Chauvet, P. Remaud-Le Saëc, M. Bourgeois, N. Chouin, L. Rbah-Vidal, R. Tripier, F. Haddad, F. Kraeber-Bodéré, C. Bodet-Milin and M. Chérel, *Int. J. Mol. Sci.*, 2019, **20**, 2564.
42 S. Gouard, C. Maurel, S. Marionneau-Lambot, D. Dansette, C. Bailly, F. Guérard, N. Chouin, F. Haddad, C. Alliot, J. Gaschet, R. Eychenne, F. Kraeber-Bodéré and M. Chérel, *Cancers*, 2020, **12**, 2721.
43 F. Bassal, J. Champion, S. Pardoue, M. Seydou, A. Sabatié-Gogova, D. Deniaud, J.-Y. L. Questel, G. Montavon and N. Galland, *Inorg. Chem.*, 2020, **59**, 13923–13932.
44 P. A. Cox, A. G. Leach, A. D. Campbell and G. C. Lloyd-Jones, *J. Am. Chem. Soc.*, 2016, **138**, 9145–9157.
45 P. A. Cox, M. Reid, A. G. Leach, A. D. Campbell, E. J. King and G. C. Lloyd-Jones, *J. Am. Chem. Soc.*, 2017, **139**, 13156–13165.
46 J. Spetz, N. Rudqvist and E. Forssell-Aronsson, *Cancer Biother.Radiopharm.*, 2013, **28**, 657–664.
47 R. H. Larsen, S. Slade and M. R. Zalutsky, *Nucl. Med. Biol.*, 1998, **25**, 351–357.
48 S. Lindegren, T. Bäck and H. J. Jensen, *Appl. Radiat. Isot.*, 2001, **55**, 157–160.
49 M. Bourgeois, F. Guérard, C. Alliot, M. Mougin-Degraef, H. Rajerison, P. Remaud-Le Saëc, J.-F. Gestin, F. Davodeau, M. Chérel, J. Barbet and A. Faivre-Chauvet, *J. Labelled Compd. Radiopharm.*, 2008, **51**, 379–383.